

# Uncertainty-Aware Capacity Allocation in Flow-Based Market Coupling

Richard Weinhold<sup>a,1,\*</sup>, Robert Mieth<sup>b,1</sup>

<sup>a</sup>*Faculty VII Economics and Management, TU Berlin, 10623 Berlin, Germany*

<sup>b</sup>*Department of Electrical and Computer Engineering, Tandon School of Engineering,  
New York University, New York, NY 10012 USA*

---

## Abstract

The effective allocation of cross-border trading capacities is one of the central challenges in implementation of a pan-European internal energy market. Flow-based market coupling (FBMC) has shown promising results for to achieve better price convergence between market areas, while, at the same time, improving congestion management effectiveness by explicitly internalizing power flows on critical network elements in the capacity allocation routine. However, the question of FBMC effectiveness for a future power system with a very high share of intermittent renewable generation is often overlooked in the current literature. This paper provides a comprehensive summary on FBMC modeling assumptions, discusses implications of external policy considerations and explicitly discusses the impact of high-shares of intermittent generation on the effectiveness of FBMC as a method of capacity allocation and congestion management in zonal electricity markets. We propose to use an uncertainty model of renewable energy injections and probabilistic security margins on the FBMC parameterization to effectively assess the impact of forecast errors in renewable dominant power systems. Numerical experiments on the well-studied IEEE 118 bus test system demonstrate the mechanics of the studied FBMC simulation. Our data and implementation are published through the open-source Power Market Tool (POMATO).

*Keywords:* Flow-based market coupling, zonal electricity markets, optimal power flow, chance constraints, flow reliability margins

---

\*Corresponding author

*Email addresses:* [riw@wip.tu-berlin.de](mailto:riw@wip.tu-berlin.de) (Richard Weinhold),  
[robert.mieth@nyu.edu](mailto:robert.mieth@nyu.edu) (Robert Mieth)

<sup>1</sup>R. Weinhold and R. Mieth contributed equally to this work. The order of authorship has been chosen based on the amount of RAM in the authors' workstations.

Table 1: Nomenclature.

<b>A. Sets</b>	
$\mathcal{T}$	Set of time steps within the model horizon.
$\mathcal{G}$	Set of generators.
$\mathcal{R}$	Subset $\mathcal{R} \subset \mathcal{G}$ of intermittent generators.
$\mathcal{N}$	Set of network nodes.
CNEC	Set of critical network elements and contingencies.
$\mathcal{Z}$	Set of bidding zones.
<b>B. Variables</b>	
$G_t$	Active power generation at $t \in \mathcal{T}$ indexed by $G_{g,t}, g \in \mathcal{G}$
$C_t$	Curtailment $t \in \mathcal{T}$ .
$I_t$	Active nodal power injection at $t \in \mathcal{T}$ .
$NP_t$	Zonal net-positions at $t \in \mathcal{T}$ .
$EX_t$	Bilateral exchange at $t \in \mathcal{T}$ indexed by $EX_{t,z,z'}, z, z' \in \mathcal{Z}$
$G_t^{red}$	Active power redispatch at $t \in \mathcal{T}$ .
$\alpha_t$	Generator response at $t \in \mathcal{T}$ indexed by $\alpha_{g,t}, g \in \mathcal{G}$
$T_{j,t}$	Standard deviation of the flow $t \in \mathcal{T}$ on $j \in \text{CNEC}$ .
<b>C. Parameters</b>	
$d_t$	Nodal load at $t \in \mathcal{T}$ .
$r_t$	Available intermittent generation at $t \in \mathcal{T}$
$m$	Mapping of generators/load (subscript) to nodes/zones (superscript).
$\bar{g}$	Upper generation limit.
$\bar{f}$	Line capacity of CNEC indexed as $\bar{f}_j, j \in \text{CNEC}$
$f_{j,t}^{ref}$	Reference flow on $j \in \text{CNEC}$ at $t \in \mathcal{T}$ .
$ntc$	Net-transfer capacity indexed by $ntc_{z,zz}, z, z' \in \mathcal{Z}$
$g^{da}$	Day-ahead scheduled generation at $t \in \mathcal{T}$ .
$c^{da}$	Day-ahead scheduled curtailment at $t \in \mathcal{T}$ .
$\omega_t$	Real-time deviation on intermittent generation $r_t$ at $t \in \mathcal{T}$ .
$\Omega$	Uncertainty space $\omega \in \Omega$
$\epsilon$	Risk-level
$\Phi$	Cumulative distribution function of the standard normal distribution
$\Sigma_t$	Variance-Covariance matrix of $\omega$ at $t \in \mathcal{T}$ .

## 1. Introduction

In the interconnected European power system, transnational electricity trading promises to improve system efficiency, market liquidity and price convergence (Schönheit et al., 2021c). However, the transport capacity between national market areas is limited and depends on power flow physics. Flow-based market coupling (FBMC) has been introduced as a method to compute these capacities such that cross-border trade is as unconstrained as possible, while ensuring system security and operational efficiency. FBMC addresses many deficiencies of previous capacity allocation methods (e.g., net-transfer capacities) by modeling the relationship between forecast market outcomes, the expected generator dispatch supporting this market outcome, and the resulting physical power flow through critical transmission equipment. However, the models and forecasts underlying the FBMC process are, by nature, imperfect. Additional real-time congestion management, e.g., out-of-market generator redispatch, is required to continuously ensure system security. These real-time corrections are a central aspect of the overall economic evaluation of FBMC and their importance is amplified in a power system with predominantly intermittent renewable power production and declining dispatchable generation capacities. Hence, while the benefits of FBMC have been convincingly demonstrated for today's portfolio of generation assets, its effectiveness for future renewable-dominant power system is subject of an ongoing debate among market participants, regulators and research scholars. This paper contributes to the currently scarce literature on FBMC in a highly renewable power system as follows. First, we describe a fundamental model of FBMC based on publicly available documentation. Here, we clearly distinguish between modeling choices that define the parameters of the FBMC process and the required simulation of the market-clearing and real-time dispatch processes. Second, we propose a modeling approach that internalizes statistical information of renewable generation forecasts into the FBMC routine. This allows to substitute ad-hoc fixed security margins for a higher fidelity model that more closely matches current system operator practices and requirements. Third, we demonstrate our models and implementation on the IEEE 118-bus test bed and discuss FBMC efficiency in comparison to two benchmarks. All data and code is accessible in a documented open-source repository.

### 1.1. *Background and related literature*

The European electricity system is a collection of national zonal electricity markets. The development of a European internal energy market (IEM)

aims to establish a pan-European electricity trading platform under a policy triangle of security of supply, affordability, and sustainability (European Commission, 1997). Organizing the vast majority of Europe's electricity consumption in a coordinated market framework is the achievement of over 20 years of continuous policy iteration for more effective market designs and procedures (Glachant, 2010). Central to these market coupling procedures are capacity allocation and congestion management routines, i.e., methods to determine exchange capacities between market areas such that transnational trade volumes are high, while secure system operation is guaranteed. While development of efficient methods for capacity allocation and congestion management in the early stages of the IEM were motivated by the scarcity of transmission capacity inherited from pre-liberalized market structures (Meeus and Belmans, 2008), current developments are driven by the system's transformation towards a sustainable energy system (Directorate General for Energy, 2019). Specifically, in the context of a generation portfolio that is characterized by more intermittent renewable energy sources and fewer dispatchable generators, increasing cross-border cooperation promises a more efficient utilization of available infrastructure by improving the coordination of (flexible) generation resources.

To date, various market coupling methods are in use. While most neighbouring market zones rely on net transfer capacity (NTC) or available transfer capacity (ATC), Central Western Europe (CWE), comprising France, Belgium, Luxembourg, Netherlands, Germany and Austria, has adopted the target method FBMC.

FBMC differs from NTC and ATC in how transmission capacity is allocated to markets. NTC and ATC are independent limits on the allowable exchange between two adjacent market areas and reflect the physical capacity of the transmission lines between those areas minus some security margins. This approach, however, ignores interdependencies of cross-border flows caused by the physics of power flow in an interconnected network. FBMC, on the other hand, derives limits on the net-exports (so called “net-positions”) of all involved bidding zones *simultaneously* and, thus, can capture interdependencies between trading activities and power flows more holistically for the entire coupled market. As a result, physical transmission constraints imposed by limited thermal line capacities are better reflected in the market clearing solution, while, at the same time, high cross-border trade capacity is ensured. This promises more efficient capacity allocation and improved price convergence between the zones (Schönheit et al., 2021c).

Although FBMC was inaugurated only in 2015 as part of EC Directive 15/1222 (European Commission, 2015), it was conceived and designed already decade earlier IEM (ETSO, 2001). As a result, FBMC was motivated

by necessary improvements to capacity allocation in the IEM and not by a need to realize policy targets, e.g., accommodate high shares of renewable energy sources (RES). Yet, policy specifications are applied to FBMC regulations. For example, as part of the Clean Energy Package (Directorate General for Energy, 2019) and the accompanying update to the regulation on capacity allocation and congestion management, European Commission (2019a) requires transmission system operators (TSOs) to allocate a minimal share of physical line capacity to the market. This kind of engagement with specifics of the process illustrates the regulatory willingness to closer engage with market design to bring the process in line with sustainability targets. Therefore, FBMC, as an important part of the IEM, should become an active element of the transformation process towards a decarbonized energy system.

For any policy developments, quantitative analyses of the FBMC process are an important basis, as they provide reliable context for necessary design decisions. Initial publications on FBMC stem from conceptional documentations of the involved TSOs and power exchanges (ETSO, 2001; ETSO and EuroPEX, 2004). As part of a “dry-run”, i.e., simulated operation, in 2008 (Amprion et al., 2011) and a parallel run in 2013 (Rte et al., 2015) the process was evaluated and its effectiveness in achieving higher welfare and improving price convergence was verified. Additionally, FBMC is described in a continuously updated documentation by the involved TSOs that is currently available as version 5 (50Hertz et al., 2020). Complementary descriptions and research of the involved parameters was published in different articles from TSO work-groups (Schavemaker et al., 2008; Aguado et al., 2012; Marien et al., 2013).

Independent academic publications on FBMC have mainly focused on the question on how the process can be modeled accurately and how model assumptions and parameter choices affect market outcomes and system operations. For example, Byers and Hug (2020) provide insights on the fundamental FBMC modeling process and performs a numerical sensitivity analyses for the various modeling parameters. Schönheit et al. (2020); Finck et al. (2018) evaluate the impact of different generation shift keys, a core parameter that captures the participation of generators in the zonal market outcome and, thus, maps market outcomes to power flows on selected network elements. Schönheit et al. (2021a) discuss the selection of these network elements in the context of market zone configurations.

### *1.2. Motivation and Contribution*

The above mentioned publications focus on specific modeling and parameter choices. However, they do not discuss the ability of FBMC to accommodate policy goals and the impact of a renewable-dominated generation mix.

In Schönheit et al. (2021c) the authors describe the TSOs' degree of freedom to influence FBMC parametrization and, thus, influence market results. The analysis also includes a scenario with a moderate increase in RES capacities on a synthetic test system. Matthes et al. (2019) analyse FBMC in for the target year 2025 with higher shares of RES, but the implications on FBMC are not discussed.

Realizing the importance of FBMC for the European electricity sector and motivated by the literature gap outlined above, this paper makes the following contributions.

1. Based on the actually implemented FBMC process as reported by 50Hertz et al. (2020), we derive the fundamental relationship between, FBMC parameters and market outcomes. Using this relationship, we highlight how FBMC can accommodate specific policy goals, i.e., related to trading volumes.
2. To better capture the forecast uncertainty introduced by large numbers of RES, we propose an uncertainty-aware approach to modeling FBMC. This approach is in line with risk evaluation techniques currently employed by TSOs and resembles the idea of generation shift keys. We show, that this approach produces more accurate security margins on critical network elements and improves FBMC efficiency for renewable-dominant electricity markets.
3. We evaluate the effectiveness of FBMC with and without the proposed uncertainty-aware modification by benchmarking it against capacity allocation via NTC/ATC. All data and code is published and available open-source.

## 2. FBMC Concept and Simulation

FBMC is a three-stage process designed to allocate commercial exchange capacity between adjacent electricity markets (i.e., cross-border exchange). It is coordinated by the local TSOs and power exchange and aims to accommodate inter-zonal electricity trading with respect to available transmission system capacity and physical power flows. Fig. 1 provides an overview of the three FBMC stages and shows their timing, involved stakeholders, parameters and results. For any given day  $D$ , the FBMC process starts two days in advance at  $D - 2$ , with the calculation of the so called *basecase*. The basecase is informed by TSO-generated forecasts on the expected point-of-dispatch and provides “*a best estimate of the state of the [...] system for day  $D$* ” (50Hertz et al., 2020, p. 26). Based on these forecasts, on additional predefined policies and on regulatory constraints (see discussion below), the TSOs calculate the so called *flow-based parameters* that are used to constrain the commercial exchange in the following *market clearing* stage. Generation and load bids collected from all bidding areas that are part of the CWE region are cleared in the day-ahead (DA) and intraday markets at  $D - 1$  and  $D - 0$ , respectively. Lastly, during the *re-dispatch* stage, the TSOs may require changes to the generators’ final point-of-dispatch to resolve any network congestion or other threats to system security due to real-time conditions (e.g., load and RES injections).

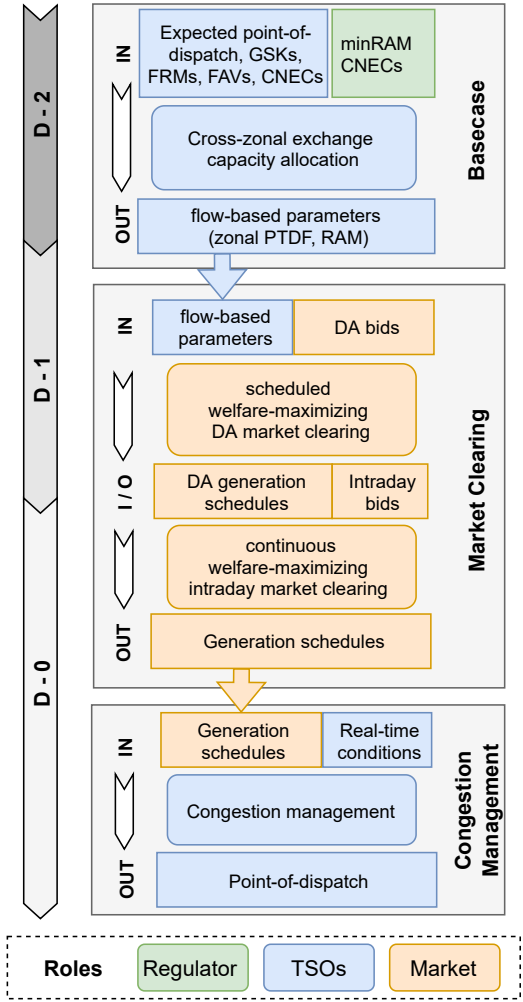


Figure 1: FBMC process overview.

## 2.1. Preliminaries

The FBMC process and the definition of the flow-based parameters relies on a model of the physical transmission system, which we formalize as follows. Consider an interconnected transmission network with  $n$  nodes and  $l$  lines. Further, let each node  $i$  be defined by its net power injection  $I_i$  collected in column vector  $I = [i_i]_{i=1}^n \in \mathbb{R}^n$ . If  $I_i > 0$ , then node  $i$  is a net generator, if  $I_i < 0$ , then node  $i$  is a net load. For each vector  $x$  there exists exactly one corresponding vector  $f = [f_j]_{j=1}^l \in \mathbb{R}^l$  that collects the flows along each line  $j$  and is defined by the physics of power flow in a network. The maximum allowable flow (capacity) of each line  $j$  is given by  $\bar{f}_j$  collected in vector  $[\bar{f}_j]_{j=1}^l$ . Power flow physics in high-voltage transmission networks allow a linear approximation of the relationship between  $f$  and  $I$  using a *power transfer distribution factor* matrix  $\text{PTDF} \in \mathbb{R}^{l \times n}$  such that

$$f = \text{PTDF} \cdot I. \quad (1)$$

See, e.g., Weinhold and Mieth (2020a) for a more detailed derivation. Further, assume that the nodes of the network are grouped in  $z$  compact *market zones* such that each zone  $k$  collects nodes  $\mathcal{N}_k$  and  $\bigcup_{k=1}^z \mathcal{N}_k = \{1, \dots, n\}$  and  $\bigcap_{k=1}^z \mathcal{N}_k = \emptyset$ . The set of all zones is denoted as  $\mathcal{Z}$  and the sum of the injections of all nodes in one zone is called the *net-position*  $np_k$  of zone  $k$  collected in vector  $np \in \mathbb{R}^z = [np_k]_{k=1}^z$ . If  $np_k > 0$ , then zone  $k$  is a net exporter and if  $np_k < 0$ , then zone  $k$  is a net importer.

## 2.2. Flow-based formalism

The effectiveness of FBMC to enable least-cost, yet physically feasible day-ahead market outcomes across interconnected market zones hinges on the precise definition of the flow-based parameters, which specify (i) how cross-border power exchange affects power flow on transmission lines and (ii) how much capacity on each line is available to accommodate flow caused by cross-border exchange. Each specification (i) and (ii) is given by the following respective parameter:

- (i) **Zonal PTDF**; Zonal  $\text{PTDF}^z \in \mathbb{R}^{l' \times z}$  maps net-position vector  $np$  to the flow on a *selection* of  $l' \leq l$  lines in the network, the so called *critical network elements* (CNE).
- (ii) **Remaining available margin (RAM)**; For each CNE, vector  $\text{RAM} \in \mathbb{R}^{l'}$  defines the absolute capacity that is available for cross-border trading in the day-ahead market.

Although these parameters are generated, exchanged and published following specific rules requested by regulation and laid out in the documentation of

the FBMC process in 50Hertz et al. (2020), they depend on the exact choice of the underlying forecast and meta-parameters that are either chosen at the discretion of the TSOs or given by policy requirements.

First, the exact definition of  $\text{PTDF}^z$  depends on the chosen CNEs, additional contingency scenarios and so called *generation shift key (GSK)*.

- **CNE/CNEC:** “*A CNE is considered to be significantly impacted by CWE cross-border trade, if its maximum CWE zone-to-zone PTDF is larger than a threshold value that is currently set at 5%.*”

(50Hertz et al., 2020, p. 19f)

Network elements are considered CNE only if TSOs determine that their flow is significantly driven by cross-zonal exchange. This selection prevents heavily loaded lines that are largely insensitive to changes in the zones’ net-positions to limit inter-zonal exchange capacity allocation. Further, for each network element the TSOs identify a set of contingencies (C), i.e., unplanned outages of network elements, that highly impact the flow on said CNE. The resulting set of critical network elements and contingencies (CNECs), the full PTDF matrix and additional linear outage factors, which capture flow shifts during the selected contingencies, form the basis for  $\text{PTDF}^z$  computation.

- **GSKs:** “*A GSK aims to deliver the best forecast of the impact on Critical Network Elements of a net-position change [and] is calculated according to the reported available market driven power plant potential of each TSO divided by the sum of market driven power plant potential in the bidding zone.* ”.

(50Hertz et al., 2020, p. 38ff)

Since line flows  $f$  depend on the injection at every node, the computation of  $\text{PTDF}^z$  requires an estimation of how changes in net-position  $np$  are distributed to changes in net injections  $I$ . Assuming that the difference between forecasted net-position in the basecase and the realized net-position in the market phase is small, the set of generators that will serve this difference by “shifting” their production levels can be anticipated. The resulting nodal contribution to net-position changes is formally captured in vector  $\text{GSK} \in \mathbb{R}^{n \times z}$  that maps a change  $\Delta np$  in net-positions to a change in nodal injections  $\Delta I$  such that

$$\Delta I = \text{GSK} \Delta np, \quad (2)$$

which further provides a clearer definition of  $\text{PTDF}^z$  as

$$\text{PTDF}^z = \text{PTDF} \cdot \text{GSK}. \quad (3)$$

Note that this approach implicitly attributes all possible changes to net-position  $np$  to changes of dispatchable generators and is ignorant to  $np$  changes caused by forecast errors of load and RES.

Second, the final RAM value can be corrected by additional *flow reliability margins* (FRMs) and *final adjustment values* (FAVs).

- **FRM:** “[F]or each Critical Network Element, a Flow Reliability Margin (FRM) has to be defined, that quantifies at least how [...] uncertainty impacts the flow on the Critical Network Element.”

(50Hertz et al., 2020, p. 47)

FRMs are static RAM reductions that are informed by past observations on how the flow on each CNE changed between the baseload forecast and the point-of-dispatch realization. Therefore, FRM captures forecast uncertainty of load and RES injections.

- **FAV:** “With the Final Adjustment Value (FAV), operational skills and experience that cannot be introduced into the Flow Based-system can find a way into the Flow Based-approach by increasing or decreasing the remaining available margin (RAM) on a CNE for very specific reasons [...] to eliminate the risk of overload on the particular CNE.”

(50Hertz et al., 2020, p. 25)

FAVs decrease or increase RAM based on the operational experience of the TSOs. It may reflect remedial actions at the point of dispatch or other complex system security considerations.

Finally, the available commercial exchange capacity between market zones is defined by constraining the zonal net-positions *relative to the baseload*. For the baseload, the TSOs forecast the expected flow  $f^{bc}$  on all CNEs and the expected net-positions  $np^{bc}$ . The net-positions that can be realized during the market stage ( $np^{da}$ ) can only differ from  $np^{bc}$  if CNE limits  $\bar{f}$  (corrected by FRMs and FAVs) are maintained:

$$\text{PTDF}^z(np^{da} - np^{bc}) \leq \bar{f} - (\text{FRM} + \text{FAV}) - f^{bc}. \quad (4a)$$

Note that the explicit introduction of  $np^{bc}$  in (4a) is necessary to ensure the validity of the GSKs and, thus,  $\text{PTDF}^z$ . See also Schönheit et al. (2020) for a broader discussion. Eq. (4a) can be rewritten as follows:

$$\text{PTDF}^z \cdot np^{da} \leq \bar{f} - (\text{FRM} + \text{FAV}) - f^{bc} + \text{PTDF}^z \cdot np^{bc} \quad (4b)$$

$$\Leftrightarrow \text{PTDF}^z \cdot np^{da} \leq \bar{f} - (\text{FRM} + \text{FAV}) - f^{ref} \quad (4c)$$

$$\Leftrightarrow \boxed{\text{PTDF}^z \cdot np^{da} \leq \text{RAM}.} \quad (4d)$$

In Eq. (4c),  $f^{ref} = f^{bc} - \text{PTDF}^z \cdot np^{bc}$  denotes the *reference flow* that captures a residual between the parameter choices made in  $\text{PTDF}^z$  and the forecasted  $f^{bc}$ . While  $f^{ref}$  can be assumed small, it is not necessarily zero. Eq. (4d) yields the desired limit on market-based net-positions  $np^{da}$  subject to the flow-based parameters  $\text{PTDF}^z$  and RAM (50Hertz et al., 2020, p. 60). The space of all possible net-positions that fulfill (4d) is called *flow-based domain*.

Irregardless of the formal RAM definition, regulations, e.g., the European Commission (2019a, Art. 16), prescribe specific conditions that define a minimal percentage of CNE capacity that must be made available for cross-border exchange and that ensures the feasibility of long-term traded capacities.

- **minRAM:** “*CNECs with a RAM of less than the minRAM factor multiplied by Fmax at zero-balance are assigned an AMR value (adjustment for minRAM) in order to increase the RAM.*”

(50Hertz et al., 2020, p. 64)

The minRAM criterion defines a lower bound for the RAM based on the CNEs capacity and is applied after FRMs and FAVs:

$$\text{RAM} = \max(\text{minRAM} \cdot \bar{f}, \bar{f} - (\text{FRM} + \text{FAV}) - f^{ref}). \quad (5)$$

- **Long-term allocations:** “*the long-term-allocated capacities of the yearly and monthly auctions have to be included in the initial Flow Based-domain*”

(50Hertz et al., 2020, p. 66)

This requirement ensures that trades on energy futures and bilateral delivery contracts outside of the day-ahead or intraday market clearing stage have to be feasible within the flow-based domain.

FRMs, FAVs, minimum remaining available margin (minRAM) and long-term allocations either enlarge the flow-based domain to enable higher price convergence (minRAM), shrink the flow-based domain to accommodate security margins (FRM), or go both ways (FAV).

### 2.3. Flow based discussion

It is clear, that the resulting flow-based parameters do not only reflect formal definitions, but also methods to account for uncertainty or imperfections, e.g., arising from zonal aggregation and required forecasts. Further, their specific configuration depends on policy considerations on the desired level of restrictions on commercial cross-border exchange. Regulation states a clear goal of achieving higher price convergence (European Commission, 2019b). As a result, solely cross zonal tie lines are encouraged to be nominated as CNEs (ACER and CEER, 2018, p.8) and the a minRAM of 70% will be required by 2025. This indicates that large trading domains are desirable

and that potentially higher cost for congestion management (e.g., real-time redispatch) fall into the responsibility of local TSOs.

In previous academic studies, derivation and application of the flow-based parameters is mostly understood as a strictly formal process. Studies generally focus on the formal dimension in their numerical experiments by describing the relation of a specific parametrization policy to a chosen metric, e.g., system cost or welfare, with the goal to provide a better understanding of parameter choices. Current literature on flow-based parameter policies in relation to system cost exist for GSKs (Voswinkel et al., 2019), min-RAMs (Schönheit et al., 2021b), commercial exchange and uncertainty in the basemode parametrization (Byers and Hug, 2020) and selection of CNECs (Schönheit et al., 2021c). All contribute to better understanding the relation between the parameters, however comparability remains difficult since it requires similar definitions on how flow-based domains should be used. Most studies do not explicitly discuss which overall target the capacity allocation strives for.

Since the current regulation explicitly requires a parametrization to provide higher capacities to the markets with the goal to ensure the integration of higher shares of RES (European Commission, 2019a) it is important to make these considerations part of the modeling and academic process. Without such considerations the effectiveness of FBMC to accommodate higher shares of RES cannot be definitively answered. With this paper we aim to contribute to this discussion by providing a transparent parametrization of the FBMC process and the underlying market simulations and by numerically show the effects of higher shares of RES. We explicitly discuss different consideration regarding the permissiveness of day-ahead trading domains by minRAM and CNEC selection and the effect on total system cost and congestion management. In addition we provide a sensible way to include risk-aware security margins FRMs in the modeling process. The permissive capacity allocation in systems with high shares of intermittent generation raises the question of operability. Thus we include process-considerations regarding expected deviations from scheduled generation to make the system more robust.

### 3. Model Formulation

#### 3.1. Market Simulation

In addition to computing flow-based parameters, modeling and studying the three-step FBMC process as shown in Fig. 1 requires a simulation of basemode, market clearing and congestion management processes. We model all of these steps as a multi-period economic dispatch (ED) problem, where

each step is constrained by a specific set of network or transport constraints. The ED is given as:

$$\min \sum_{t \in \mathcal{T}} c(G_t) + p(e^T C_t) \quad (6a)$$

$$\text{s.t.} \quad 0 \leq G_t \leq \bar{g} \quad \forall t \in \mathcal{T} \quad (6b)$$

$$0 \leq C_t \leq r_t \quad \forall t \in \mathcal{T} \quad (6c)$$

$$m^n G_t + m^n(r_t - C_t) - d_t = I_t \quad \forall t \in \mathcal{T} \quad (6d)$$

$$m^z G_t + m^z(r_t - C_t) - m^z d_t = NP_t \quad \forall t \in \mathcal{T} \quad (6e)$$

$$NP_{t,z} = \sum_{z' \in \mathcal{Z}} EX_{t,z,z'} - EX_{t,z',z} \quad \forall t \in \mathcal{T}, \forall z \in \mathcal{Z} \quad (6f)$$

$$e^T I_t = 0 \quad \forall t \in \mathcal{T} \quad (6g)$$

where  $t$  indicates the market clearing time steps (e.g., hour or 15 minutes) and  $\mathcal{T}$  is the set of times steps. Objective function (6a) minimizes system cost given by the cost of generation  $c(G_t)$  and the cost of curtailing RES  $pC_t$ , where  $c(\cdot)$  is a generator cost function model,  $G_t$  is the vector of generator production levels,  $C_t$  is the vector of RES curtailment,  $p$  is a scalar curtailment penalty and  $e$  is the vector of ones in appropriate dimensions. Constraint (6b) enforces limits  $\bar{g}$  on generator outputs  $G_t$  and constraint (6c) limits curtailment  $C_t$  to available capacity  $r_t$ . Finally, Eqs. (6d) and (6e) balance power on a nodal and zonal resolution. Nodal energy balance (6d) defines nodal power injections  $I_t$  in terms of nodal load and generation by mapping generator and RES injections to each node via map  $m^n$ . Similarly, the zonal energy balance defines the zonal net-position  $NP_t$  as the difference between zonal load and generation mapping resources and loads into each zone via map  $m^z$ . Eq. (6f) defines auxiliary variable  $EX_{t,z,z'} \geq 0$ , which denotes the bilateral exchange from zone  $z$  to zone  $z'$ .<sup>2</sup> Eq. (6g) enforces system balance. Note that all decision variable of the model are written in capital letters, while parameters are given as lower case symbols.

Nodal power injections or zonal net-positions of ED (6) can be subject to limitations given by the transmission system capacity and chosen power flow model. Hence, FBMC-based market clearing can be modeled by using ED (6) and additionally enforcing

$$NP_t \in \mathcal{F}^z := \{x : \text{PTDF}_t^z x \leq RAM_t\} \quad \forall t \in \mathcal{T}, \quad (7)$$

---

<sup>2</sup>Note, when constraints apply to net-positions only, the  $EX$  remains unconstrained. Therefore, a small penalty factor for  $EX$  is included in the objective function to discourage excessive exchange but does not distort model results with less than 0.5% of the objective value.

where  $\mathcal{F}^z$  is the flow based domain as derived in Section 2 above. Note that the zonal PTDF may be different for each time step, indicated by index  $t$ . Alternatively, nodal market clearing, i.e., an economic dispatch that is constrained by all network transmission lines, can be modeled by constraining (6) with

$$I_t \in \mathcal{F}^n := \{x : \text{PTDF}^n x \leq \bar{f}\} \quad \forall t \in \mathcal{T}. \quad (8)$$

Nodal market clearing limits the cross-zonal exchange only implicitly by taking into account the transmission capacity of the whole network. On the other hand, we can constrain cross-zonal exchange  $\text{EX}_{t,z,z'}$  directly using static bilateral NTCs:

$$\text{EX}_t \in \mathcal{F}^{ntc} := \{x : 0 \leq x \leq ntc\} \quad \forall t \in \mathcal{T}. \quad (9)$$

Notably, the approach in (9) does not include a physical power flow model.

All FBMC steps can be modeled through (6) in combination with either (7), (8) or (9) as summarized in the FBMC column of Table 2. Notably, the basecase is a nodal market clearing, following the intuition that the basecase should resemble D-0 as well as possible. The day-ahead market is cleared zonally with flow-based parameters  $\text{PTDF}_t^z$  and RAM derived from the basecase results as per (4). D-0 congestion management again relies on a nodal network representation (8) and requires additional constraints that impose cost for deviating from the market clearing results:

$$C(G^{red}) = c^{red} \sum_{t \in \mathcal{T}} |G_t^{red}| \quad (10a)$$

$$G_t - g_t^{da} = G_t^{red} \quad \forall t \in \mathcal{T} \quad (10b)$$

$$C_t \geq c^{da} \quad \forall t \in \mathcal{T}, \quad (10c)$$

Table 2: Model configuration for FBMC, Nodal and NTC market clearing.

	<b>FBMC</b>	<b>NTC</b>	<b>Nodal</b>
D-2: Basecase	(6a) s.t. (6b)–(6g), (8)	–	–
D-1: Market Clearing	(6a) s.t. (6b)–(6g), (7)	(6a) s.t. (6b)–(6g), (9)	(6a) s.t.
D-0: Congestion Management		(6a)+(10a) s.t. (6b)–(6g), (8), (10b), (10c)	(6b)–(6g), (8)

where  $g_t^{da}$  and  $c_t^{da}$  are the decisions on  $G_t$  and  $C_t$  from the previous market clearing stage. Note that we do not explicitly model an intraday market stage and, for now, assume that load and RES injections do not change between the market stage and the real-time point of dispatch.

For reference, zonal market clearing using static bilateral NTCs and a nodal market clearing are modeled and their resulting formulations are itemized in Table 2 as well. The NTC market clearing is modeled in two steps, because it does not require a baseload computation. The necessary congestion management step is the same as for FBMC. The nodal market is a one-shot optimization of (6) subject to nodal power flow constraints (8). Notably, the nodal market does not require a congestion management stage, because generation and network are co-optimized.

### 3.2. Probabilistic FRMs via Chance Constraints

The formulations of the previous section model FBMC under perfect foresight of load and RES injections. The intention to provide efficient commercial exchange capacities to the market in combination with high shares of intermittent renewable generation poses the question of operability and how the forecasting characteristics of the baseload can be used to robustify results against RES uncertainty. As outlined in Section 2 above, the FBMC concept recognizes the existence of forecast uncertainties in the baseload by introducing FRMs, which are tuned based on historical data and TSO-defined *risk levels* (50Hertz et al., 2020, Fig. 4-2). Specifically, TSOs use historical data to estimate the  $(1 - \epsilon)$ -percentile of the absolute deviation between forecasted baseload flows  $f^{bc}$ , corrected by changes in the market schedule, and the realized real-time flows. By setting FRMs to at least the value of this  $(1 - \epsilon)$ -percentile, TSOs ensure that lines are not overloaded due to RES or load forecast errors with a probability of  $(1 - \epsilon)$ . Thus,  $\epsilon$  defines the risk level and is usually chosen small (e.g., 1 – 5%).

To date, studies on FBMC have not considered FRMs in terms of an uncertainty model and risk-threshold, but rather employ fixed security margins that are applied uniformly to all CNEs, see e.g., Schönheit et al. (2021b,c); Wyrwoll et al. (2019). While such simplifications may be motivated by a lack of historical data to simulate the FRM computation process prescribed by regulation, ignoring the specific impact of real-time control actions caused by intermittent renewable injections may obstruct a clear assessment of the effectiveness of FBMC in high RES systems. As an alternative, we propose to model risk-aware FRMs that explicitly internalize an RES uncertainty model and the impact of real-time generator control actions on each CNE. To this end, instead of creating an empirical uncertainty model of the flow forecast error on each CNE, we rely on a parameterized RES forecast error

distribution and control participation factors. This approach leverages results on chance-constrained optimal power flow first proposed by Bienstock et al. (2014).

We model the uncertain injection from RES generators as  $r_t(\omega) = r_t + \omega_t$ , where  $\omega_t$  is a zero-mean random vector that captures the forecast error of renewable generation  $r_t$ . We assume that the distribution can be modeled as a normal distribution such that  $\omega_t \sim N(0, \Sigma_t)$ , where  $\Sigma_t$  denotes the covariance matrix of  $\omega_t$ . Following the empirical results of Dvorkin et al. (2016), we will rely on the assumption that  $\omega_t$  is normally distributed for the remainder of this paper, but note that the proposed approach can be modified to accommodate different distributional assumptions, see e.g., Roald et al. (2015); Dvorkin (2020). Next, we realize that, because the basecase and day-ahead markets are cleared based on forecast  $r_t$ , error  $\omega_t$  creates a system imbalance and assume that the systems reaction to this imbalance can be anticipated. Similar to how GSKs capture the estimated distribution of  $\Delta np$  to all generators, we introduce vector of control participation factors  $\alpha_t$  that maps the reaction of generators to imbalance  $\omega_t$  as:

$$G_t(\omega_t) = G_t - \alpha_t(e^T \omega_t). \quad (11)$$

Since  $\omega_t$  and, thus,  $G_t(\omega_t)$  are random variables, we first formulate the zonal ED as a probabilistic problem

$$\begin{aligned} \min \quad & \mathbb{E}[C(G(\omega))] \\ \text{s.t.} \quad & \end{aligned} \quad (12a)$$

$$\mathbb{P}[0 \leq G_{g,t}(\omega) \leq \bar{g}_g] \geq 1 - \epsilon \quad \forall t \in \mathcal{T}, \forall g \in \mathcal{G} \quad (12b)$$

$$\mathbb{P}[\text{PTDF}_{j,t}^z \cdot NP_t(w) \leq \bar{f}_j - f_{j,t}^{\text{ref}}] \geq 1 - \epsilon \quad \forall t \in \mathcal{T}, \forall j \in \text{CNEC} \quad (12c)$$

$$m_g^z G_t(\omega) + m_r^z r_t(\omega) - C_t - d_t = NP_t(w) \quad \forall t \in \mathcal{T}, \forall \omega \in \Omega. \quad (12d)$$

Objective (12a) minimizes the expected system cost. Constraints (12b) and (12c), ensure that the probability that a generator can fulfill its required response  $\alpha_t(e^T \omega_t)$  or a CNEC is not overloaded is at least  $(1 - \epsilon)$ . These so called *chance constraints* resemble the value-at-risk, a risk metric commonly used in the finance industry (Bienstock et al., 2014). Lastly, Eq. (12d) ensures that the system is balanced for all possible outcomes of  $\omega \in \Omega$ .

Problem (12) can not be solved directly, but allows a computationally tractable deterministic reformulation. First, recall that  $\omega_t$  is zero mean, i.e.,  $\mathbb{E}[\omega_t] = 0$ . For a linear cost function model  $c(G)$  we therefore get  $\mathbb{E}[c(G(\omega_t))] = c(G(\omega_t))$ . See, e.g., Mieth et al. (2020) for the derivations for quadratic cost functions. Next, chance-constraints (12b) and (12c) can

be reformulated by recalling that for any random vector  $x \sim N(\mu, \Sigma)$  it holds that:

$$\mathbb{P}[x \leq \bar{x}] \geq (1 - \epsilon) \Leftrightarrow \mu + \Phi^{-1}(1 - \epsilon)\sigma(x) \leq \bar{x}, \quad (13)$$

where  $\Phi$  is the cumulative distribution function of the standard normal distribution and  $\sigma(x)$  is the standard deviation of  $x$ . Using (13) to reformulate (12b) and (12c) we get:

$$\mathbb{E}[G_{g,t}(\omega_t)] = \mathbb{E}[G_{g,t} - \alpha_{g,t}(e^T \omega_t)] = G_{g,t} \quad (14)$$

$$\sigma(G_{g,t}(\omega_t)) = \sqrt{\text{Var}[\alpha_{g,t}(e^T \omega_t)]} = \sqrt{\alpha_{g,t}^2(e^T \Sigma_t e)} = \alpha_{g,t} S_t \quad (15)$$

$$\begin{aligned} \mathbb{E}[\text{PTDF}_{j,t}^z \cdot NP_t(w)] &= \mathbb{E}[\text{PTDF}_{j,t}^z(m_g^z G_t(\omega) + m_r^z r_t(\omega) - m_d^z d_t)] \\ &= \text{PTDF}_{j,t}^z(m_g^z G_t + m_r^z r_t - m_d^z d_t) \end{aligned} \quad (16)$$

$$\begin{aligned} \sigma[\text{PTDF}_{j,t}^z \cdot NP_t(w)] &= \sqrt{\text{Var}[\text{PTDF}_{j,t}^z(m_g^z G_t(\omega_t) + m_r^z r_t(\omega_t) - m_d^z d_t)]} \\ &= \sqrt{[\text{PTDF}_{j,t}(m_r^z - m_g^z \alpha e^t)] \Sigma_t [\text{PTDF}_{j,t}(m_r^z - m_g^z \alpha e^t)]^T} \\ &= \|\text{PTDF}^z(m_r^z - m_g^z \alpha e^T) \Sigma_t^{1/2}\|_2, \end{aligned} \quad (17)$$

where we define  $S_t^2 = e^T \Sigma_t e$  and  $\|\cdot\|_2$  denotes the 2-norm. Lastly, (12d) holds for all  $\omega_t$ , if the system is balanced in expectation and the sum of all control actions is exactly equal to the system imbalance, i.e.,:

$$e^T \alpha_t(e^T \omega) = e^T \omega_t \Leftrightarrow e^T \alpha_t = 1. \quad (18)$$

Thus, the deterministic reformulation of (12) is given as:

$$\min C(G(\omega)) \quad (19a)$$

$$\text{s.t. } G_t + z_\epsilon \alpha s \leq \bar{g} \quad \forall t \in \mathcal{T} \quad (19b)$$

$$-G_t + z_\epsilon \alpha s \geq 0 \quad \forall t \in \mathcal{T} \quad (19c)$$

$$\text{PTDF}_{j,t}^z \text{NP}_t \leq \bar{f}_j - f_{j,t}^{ref} - z_\epsilon T_{j,t} \quad \forall t \in \mathcal{T}, \forall j \in \text{CNEC} \quad (19d)$$

$$\|\text{PTDF}_{j,t}^z(m_r^z - m_g^z \alpha e^T) \Sigma_t^{1/2}\|_2 \leq T_{j,t} \quad \forall t \in \mathcal{T}, \forall j \in \text{CNEC} \quad (19e)$$

$$m_g^z G_t + m_r^z \hat{r}_t - m_d^z d_t = \text{NP}_t \quad \forall t \in \mathcal{T} \quad (19f)$$

$$e^T \alpha_t = 1 \quad \forall t \in \mathcal{T} \quad (19g)$$

where we use  $z_\epsilon = \Phi^{-1}(1 - \epsilon)$  for a more concise notation and introduce auxiliary variable  $T_{j,t}$  to denote the standard deviation of the flow across CNEC  $j$ . Constraint (19e) is a second-order conic constraint, which is convex and can be solved efficiently by modern off-the-shelf solvers. The variable  $\alpha$  can be chosen as parameter, similarly to the GSK, or optimized as a decision

variable in (19). In this paper we use the latter approach, thus allowing for an optimized generator response. Additionally, the risk-level is defined with  $\epsilon = 5\%$  and  $\Sigma$  is calculated with an assumed standard deviation of  $10\% \cdot \hat{r}$ , that is consistent with other publications (Mieth et al., 2020; Dvorkin et al., 2016, p.29).

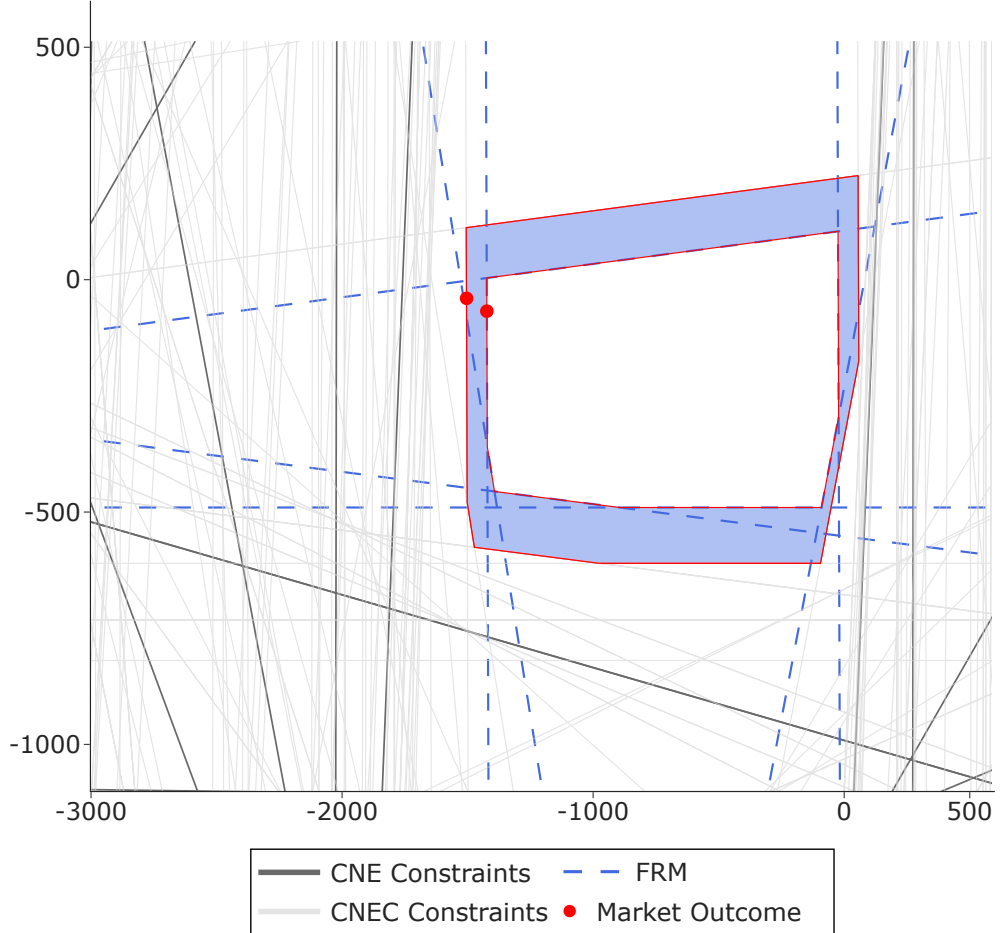


Figure 2: Flow-based domain with FRMs for exchange *Zone 1 - Zone 2* (x-axis) and *Zone 2 - Zone 3* (y-axis).

We interpret term  $z_\epsilon T_{j,t}$  in Eq. (19d) as the endogenous FRM that reduces capacity for each CNEC based on the RES uncertainty model. Fig. 2 shows the resulting impact on the flow-based domain for a single time step for exchange from *Zone 1* to *Zone 2* on the x-axis and *Zone 2* to *Zone 3* on the y-axis. See Fig. 3 in Section 4 below for an illustration of the zones. Each line in the figure corresponds to a row of the zonal power transmission distribution factor (PTDF) matrix and colored light grey for CNECs and dark

grey for CNE. The The FRMs (dashed blue) reduce the flow-based domain by the blue area. Subsequently, the market outcome (red dot) will also move inward, leading to lower commercial exchange. However, Fig. 2 shows, that the necessary margin to achieve  $(1 - \epsilon)$  security differs among CNEs, which indicates that a fixed FRM proxy margin would over- or underestimate the RAM on some CNE.

## 4. Case Study

### 4.1. Data Set

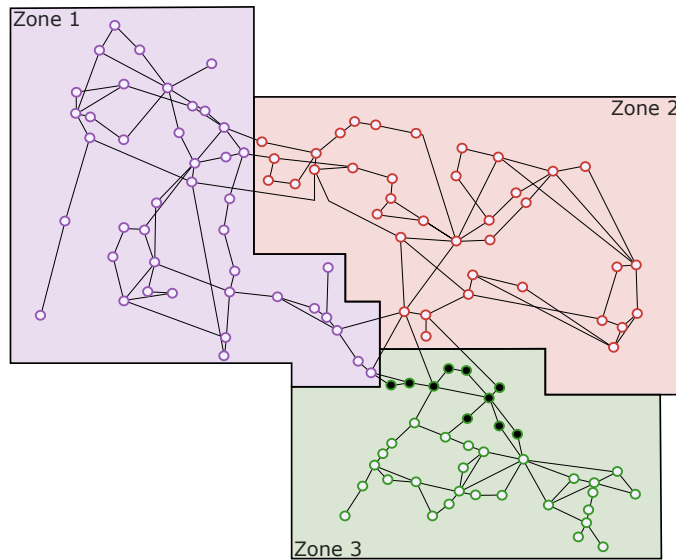


Figure 3: Topology of the IEEE 118 bus case, zones indicated by color. Changes in topology from the original data are indicated with filled nodes.

The numerical experiments build on the Pena et al. (2017) version of the IEEE-118 bus case, which augments the well known case study by additional generation technologies, zonal configuration and hourly load and RES injection timeseries for a full year. In Pena et al. (2017) the authors kept the original topology from the original IEEE-118 bus network, but line capacities are generously (4x-5x) scaled with installed capacity.

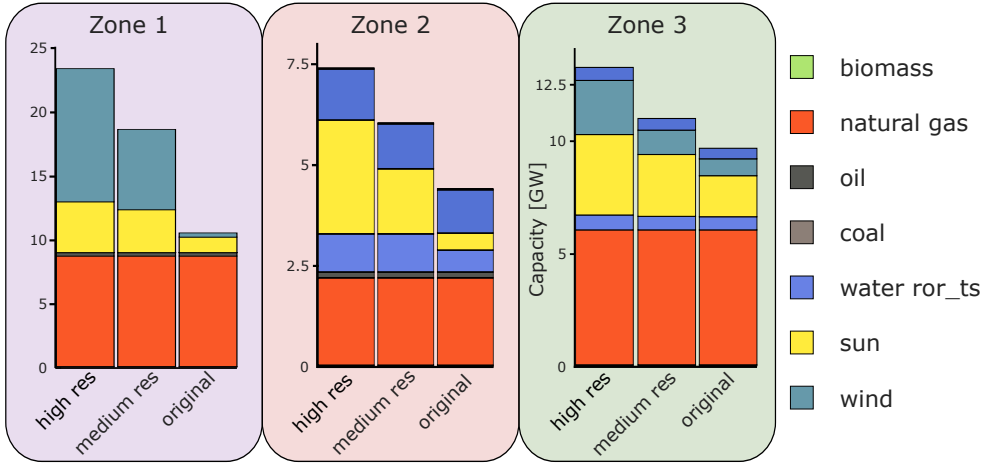


Figure 4: Installed capacities for the three scenarios *original*, *medium res* and *high res*.

The original data in Pena et al. (2017) is complemented in this study with two scenarios that further increase the share of RES generation in the total generation over the model horizon from 26% in the original data to 50% (*medium res*) and 70% (*high res*). The resulting installed capacities are itemized in Fig. 4 for the three scenarios *original*, *medium res* and *high res*. To better reflect the scarcity of transmission capacity, all line capacities are scaled down by 30%. Additionally, the zonal configuration was slightly adjusted so all zones have shared borders. This is indicated in Fig. 3 by nodes that are filled solid black, which were allocated to “Zone 2” (red) and are now allocated to “Zone 3” (green).

We analyze the effectiveness of FBMC by comparing system cost, which are composed of generation cost at the market clearing stage and additional congestion management (redispatch) in D-0. See also (10). We set the cost for redispatch to 30\$ per MWh and curtailment cost to 5\$ per MWh. Note that congestion management does not just revert a zonal solution to an optimal nodal solution, but tries to achieve a network-feasible solution with minimal deviations from the zonal solution.

#### 4.2. Zonal benchmarks

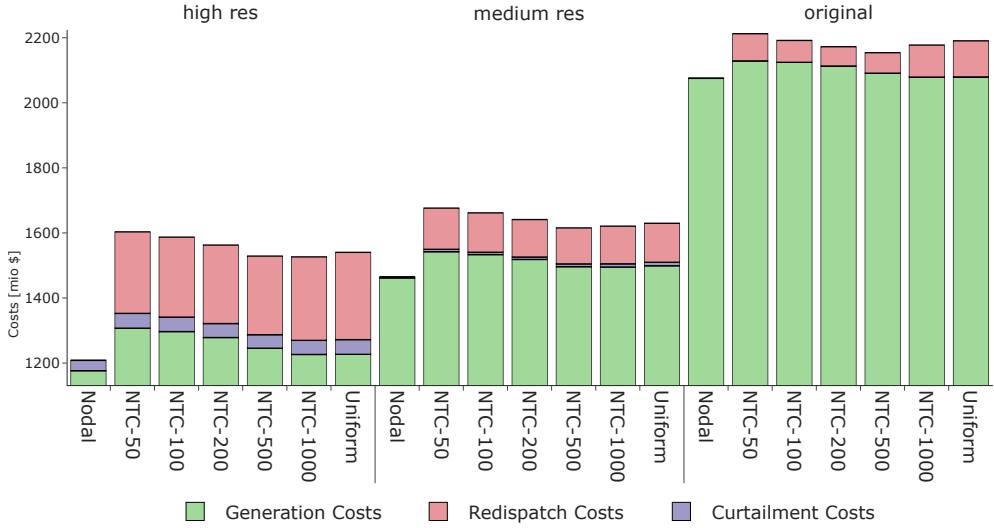


Figure 5: Cost composition of zonal NTCs market clearing and the nodal reference.

Fig. 5 shows the benchmark reference results for the three scenarios for nodal market clearing and zonal market clearing subject to NTCs. See also Table 2. System cost are evaluated after congestion management and include cost for curtailment and redispatch. The Nodal solution on the left represents the economic optimum that does not require redispatch. Zonal market clearing is shown with increasing NTCs from left to right. The “Uniform pricing“ case describes market clearing without any commercial exchange constraints.

The results show the expected pattern:

- Generation cost decrease with higher shares of cheap generation from RES.
- The nodal dispatch is the least cost solution, with no redispatch required. Additionally, due to cost for congestion management, zonal solutions often show increased generation cost.
- For zonal market clearing, more exchange capacities lead to lower generation cost. However, cost for congestion management can outweigh these savings.

Notably, an NTCs of 500 MW leads to the lowest cost dispatch for zonal market clearing. In the following, this results will be used as a benchmark for the FBMC results.

### 4.3. Flow-based parametrization

As described in Section 2.1, the flow-based parameters are used to solve the day-ahead stage in FBMC. They are composed of the zonal PTDF and RAM values and calculated from basemode generation schedules  $g^{bc}$ , power flows  $f^{bc}$  and net-positions  $np^{bc}$ . For our numerical experiments we aim to stay as close as possible to the reference given by the documented process by 50Hertz et al. (2020). We model the basemode as nodal pricing with full network representation (nodal). The zonal PTDF is composed of all cross-border lines and internal lines with a zone-to-zone PTDF value larger than 5%. Contingencies are included based on a 20% line-to-line sensitivity in case of an outage using so called load-outage distribution factors as per Jiachun et al. (2009), i.e. lines are considered contingencies that distribute 20% of line loading to the CNE. For all scenarios we use a so called *Pro-Rata* approach to calculate GSKs, i.e., changes in net-position are distributed based on the online dispatchable generation capacity at each time step (50Hertz et al., 2020; Dierstein, 2017). Consistent with current practises (Ampriion, 2019), a 20% minRAM is employed. This also ensures feasibility of (4c) as the feasible region (7) is cases where a suboptimal GSK leads to negative RAM values. The resulting FBMC configurations is denoted as *FBMC* in the following results section. To illustrate the the impact of less restrictive flow-based parameterization a second parametrization is evaluated that only considers cross-border lines as CNEs and enforces a minRAM of 70%, denoted as *FBMC<sup>+</sup>*.

All scenarios and market configurations where solved using the open Power Market Tool (POMATO) (Weinhold and Mieth, 2020b) written in Python and Julia. The calculation where done on standard PC hardware with a Ryzen 7 and 32GB of memory using the Gurobi solver (Gurobi Optimization LLC, 2018) for the deterministic configurations and the Mosek solver (MOSEK ApS, 2021) for configurations using chance constraints.

#### 4.4. Deterministic FBMC

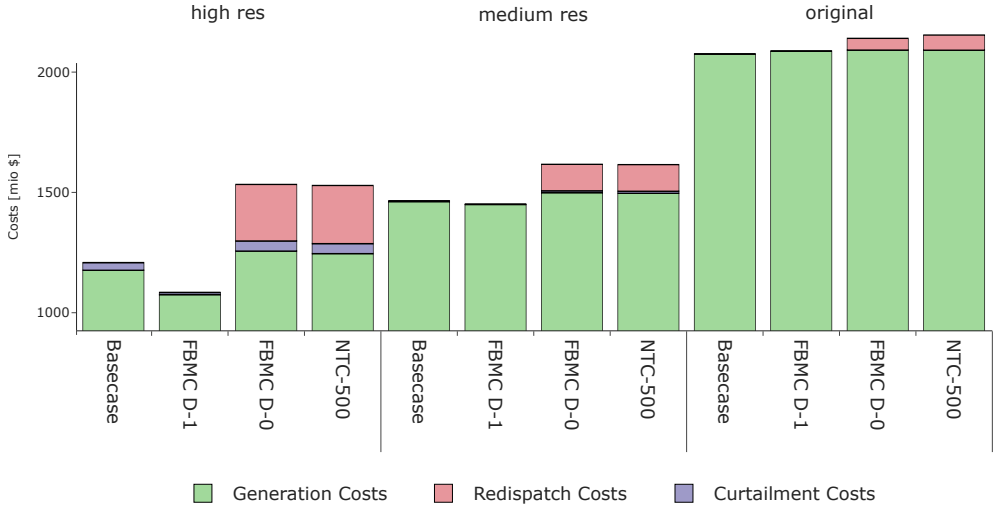


Figure 6: Cost composition of FBMC and NTC market clearing. For each scenario: Basecase, D-1 zonal market clearing and D-0 redispatch and NTC reference.

Fig. 6 shows the FBMC results for the three scenarios. The total system cost in *D-0* are also depicted in Table 3. The three market steps are depicted as *Basecase* (*D-2*), *FBMC D-1* for the day-ahead stage and *FBMC D-0* for congestion management. *NTC-500* is included as the least cost zonal reference. For each scenario the basecase represents the expected market outcome, from which the flow-based parameters are derived and used to clear the market stage. The composition of this market result shows different characteristics for the three scenarios. For the *original* data, the cost are higher compared to the nodal *Basecase*. The flow-based parameters overly constrains zonal exchange and therefore lead to sub-optimal market result, whereas for the *high res* scenario shows lower cost in the market result. The additional cost for congestion management depend on the systems ability to accommodate the market result. Here the *FBMC* and *NTC* solutions are very close, with *FBMC* generally resulting in higher generation cost, but lower cost for congestion management. Similarly to the reference results from Section 4, the NTC and FBMC solutions illustrate the trade-off between capacity allocation and congestion management, where FBMC is more restrictive and generally leads to less congestion management at higher cost in generation.

The results from the more permissive *FBMC<sup>+</sup>* configuration, which enforces a 70% minRAM and only considers cross-border CNEs, further illustrates this point. Table 3 shows the cost decomposition and Table 4

Table 3: System cost including generation and congestion management (CM) for each scenario.

		FBMC	FBMC <sup>+</sup>	NTC-500	Nodal
original	Generation	2091.45	2083.82	2091.01	2075.16
	Curtailment	0.03	0.08	0.01	0
	Redispatch	48.76	89.28	62.89	0
	total CM	48.79	89.36	62.9	0
	total	2140.24	2173.18	2153.92	2075.16
medium res	Generation	1498.85	1499.01	1496.28	1461.68
	Curtailment	7.8	9.97	8.55	3.06
	Redispatch	110	115.91	110.61	0
	total CM	117.8	125.88	119.17	3.06
	total	1616.66	1624.89	1615.44	1464.74
high res	Generation	1256.1	1239.05	1245.6	1176.48
	Curtailment	42.1	42.73	41.57	31.81
	Redispatch	234.89	243.57	241.63	0
	total CM	276.99	286.29	283.2	31.81
	total	1533.09	1525.35	1528.8	1208.29

show the respective redispatch (R), curtailment (C) and combined congestion management (sum) volumes for each scenario and include the  $FBMC^+$  configuration. Here, the  $FBMC^+$  proves less restrictive than the NTC and FBMC configurations. With the original data, the relaxed flow-based parameters  $FBMC^+$  lead to overall higher cost, due to increased congestion management. For higher shares of intermittent renewable generation, larger exchange capacities become more efficient and, while still with the higher congestion management volumes, provide the lowest cost for zonal market clearing.

Table 4: Quantities of redispatch (R) and curtailment (C) in TWh for each scenario.

	original			medium res			high res		
	C	R	C+R	C	R	C+R	C	R	C+R
FBMC	0.01	1.63	1.64	1.56	3.67	5.23	8.42	7.83	16.25
FBMC <sup>+</sup>	0.02	2.98	3	1.99	3.86	5.85	8.55	8.12	16.67
NTC-500	0	2.1	2.1	1.71	3.69	5.4	8.31	8.05	16.36
Nodal	0	0	0	0.61	0	0.61	6.36	0	6.36

#### 4.5. Probabilistic FRMs

The *high res* scenario reaches a share of intermittent renewable generation of 60 %. The dispatch of these share proves challenging when accounting for expected deviation between the day-ahead market stage and real-time. In Section 3.2 we propose a chance-constrained formulation for FRMs, that reduce the flow-based domain based on an assumed distribution of forecast errors  $\omega_t$ . The results in the previous section illustrate the trade-off between permissive capacity allocation and increased congestion management, which can be desirable depending of the associated cost. However, the cost for congestion management will change, and presumably increase, if the real-time availability is subject to forecast errors. For the numerical experiment we take a closer look at the  $FBMC^+$  scenario, as it provides the largest trading capacities and would be subject the largest impact of forecast errors.

Including FRMs, denoted as  $FBMC^+ CC$  will, in a deterministic case, lead to lower capacities allocated to the market and extension to higher cost in congestion management compared to the  $FBMC^+$  scenario without FRMs. To evaluate the impact of forecast errors that occur in real time, congestion management is run multiple times for both  $FBMC^+ CC$  and  $FBMC^+$  subject to randomized real-time deviations  $\omega$  that follow a normal distribution with a relative standard deviation of 10% from expected in-feed. The generator

response  $\alpha$ , that is an endogenous result from the chance constraint formulation, is used for both scenarios to calculate the generator response real-time deviations. The numeric results are obtained from 20 full-year runs, with hourly independent real-time deviations.

Table 5 shows that, indeed, the resulting expected cost for congestion management are indeed lower in the  $FBMC^+$   $CC$ , illustrating its higher robustness against real-time deviations. Here, we see the same values as in Table 3 with no deviations at real-time  $\omega = 0$  with  $FBMC^+$   $CC$  resulting in higher cost for congestion management. With real-time deviations  $\omega > 0$  cost for congestion management are overall lower in the  $FBMC^+$   $CC$  due to reduced exchange margins in response of expected deviations and the set generator's response.

Table 5: Cost for redispatch (R) and curtailment (C) in relation to forecast error  $\omega$ .

	$\omega = 0$			$\omega > 0$		
	C	R	C+R	C	R	C+R
$FBMC^+$	42.73	243.57	286.29	41.42	248.41	289.83
$FBMC^+ CC$	44.43	246.6	291.03	42.09	245.16	287.25

The result is visualized in Fig. 7 that visualizes the range of hourly cost for congestion management in for randomized different real-time deviations. The blue band shows the range of cost for  $FBMC^+$  and the red band show cost for  $FBMC^+$   $CC$  that includes the FRMs. The solid lines are the hourly cost without real-time deviations. The figure visualizes that, while often aligned, the  $FBMC^+ CC$  case provides a tighter band that on average provides lower cost.

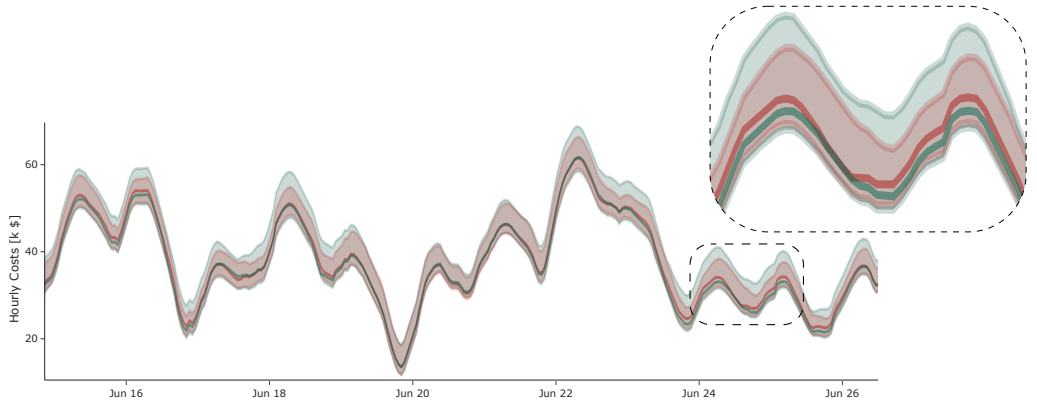


Figure 7: Range of hourly cost for congestion management for randomised real-time deviations  $\omega$  for FBMC<sup>+</sup> (blue) and FBMC<sup>+</sup> CC (red)

#### 4.6. Conclusion

In this paper we illustrate considerations necessary to model FBMC, in particular parameter choices that are policy relevant and consider high shares of intermittent renewable generation. The numerical experiments, conducted with the open power system model POMATO, highlight the effectiveness of FBMC in comparison to zonal market configurations using NTCs and quantifies the trade-off between permissive capacity allocation and increased congestion management.

Results on the extended IEEE 118 bus network of Pena et al. (2017) show, that for high shares of intermittent generation more permissive commercial exchange capacities provide the most effective configurations. Here, the additional cost for congestion management do not overcompensate lower cost in the market clearing stage. For smaller RES shares, more restrictive domains prove efficient.

With high shares of intermittent generation, the system becomes more susceptible to real-time deviation or forecast errors. We propose a chance constraint formulation that builds on the forecasting characteristics of the D-2 basecase and results in risk aware security FRMs in the day-ahead market clearing stage. Initially, the reduced commercial exchange capacity provides higher system cost but proves more robust against real-time deviations than the deterministic counter part. The proposed formulation is a suitable extension to modeling FBMC.

## Acknowledgements

The authors gratefully acknowledge the support by the German Federal Ministry for Economic Affairs and Energy (BMWi) in the project “Modellierung (De-)Zentraler Energiewenden: Wechselwirkungen, Koordination und Lösungsansätze aus systemorientierter Perspektive” (MODEZEEN, 03EI1019B)

## References

50Hertz, Amprion, APG, Creos, Elia, Rte, TenneT, TransnetBW, 2020. Documentation of the CWE FB MC Solution - Version 5.0. Technical Report.

ACER, CEER, 2018. Annual Report on the Results of Monitoring the Internal Electricity and Natural Gas Markets in 2017 - Electricity Wholesale Markets Volume. Report.

Aguado, M., Bourgeois, R., Bourmaud, J., Van Casteren, J., Ceratto, M., Jakel, M., Malfiet, B., Mestdag, C., Noury, P., Pool, M., Van Den Reek, W., Rohleder, M., Schavemaker, P., Scolari, S., Weis, O., Wolpert, J., 2012. Flow-Based Market Coupling in the Central Western European Region: On the Eve of Implementation. Technical Report C5-204. Cigré.

Amprion, 2019. Amprion Market Report 2019 - Flow Based Market Coupling: Development of the Market and Grid Situation 2015-2018. Report.

Amprion, APX-ENDEX, Belpex, Creos, Elia, EnBW, EPEX SPOT, RTE, TenneT, 2011. CWE Enhanced Flow-Based MC feasibility report.

Bienstock, D., Chertkov, M., Harnett, S., 2014. Chance-Constrained Optimal Power Flow: Risk-Aware Network Control under Uncertainty. SIAM Review 56, 461–495.

Byers, C., Hug, G., 2020. Modeling flow-based market coupling: Base case, redispatch, and unit commitment matter, in: 2020 17th International Conference on the European Energy Market, pp. 1–6.

Dierstein, C., 2017. Impact of Generation Shift Key determination on flow based market coupling, in: 2017 14th International Conference on the European Energy Market, pp. 1–7.

Directorate General for Energy, 2019. Clean Energy for All Europeans. White Paper. European Commision.

Dvorkin, Y., 2020. A chance-constrained stochastic electricity market. *IEEE Transactions on Power Systems* 35, 2993–3003.

Dvorkin, Y., Lubin, M., Backhaus, S., Chertkov, M., 2016. Uncertainty Sets for Wind Power Generation. *IEEE Transactions on Power Systems* 31, 3326–3327.

ETSO, 2001. Co-Ordinated Auctioning: A Market-Based Method for Transmission Capacity Allocation in Meshed Networks. Technical Report.

ETSO, EuroPEX, 2004. Flow-Based Market Coupling: A Joint ETSO-EuroPEX Proposal for Cross-Border Congestion Management and Integration of Electricity Markets in Europe. Technical Report.

European Commission, 1997. Directive 96/92/EC concerning common rules for the internal market in electricity.

European Commission, 2015. Commission Regulation (EU) 2015/1222: Establishing a guideline on capacity allocation and congestion management.

European Commission, 2019a. Commission Regulation (EU) 2019/943 on the internal market for electricity.

European Commission, 2019b. Directive (EU) 2019/944 on common rules for the internal market for electricity.

Finck, R., Ardone, A., Fichtner, W., 2018. Impact of Flow-Based Market Coupling on Generator Dispatch in CEE Region, in: 2018 15th International Conference on the European Energy Market, pp. 1–5.

Glachant, J.M., 2010. The Achievement of the EU Electricity Internal Market through Market Coupling. EUI Working Papers RSCAS 2010/87. Florence School of Regulation.

Gurobi Optimization LLC, 2018. Gurobi Optimizer Reference Manual.

Jiachun, G., Yong, F., Zuyi, L., Shahidehpour, M., 2009. Direct Calculation of Line Outage Distribution Factors. *IEEE Transactions on Power Systems* 24, 1633–1634.

Marien, A., Luickx, P., Tirez, A., Woitrit, D., 2013. Importance of design parameters on flowbased market coupling implementation, in: 2013 10th International Conference on the European Energy Market, Stockholm, Sweden. pp. 1–8.

Matthes, B., Spieker, C., Klein, D., Rehtanz, C., 2019. Impact of a Minimum Remaining Available Margin Adjustment in Flow-Based Market Coupling, in: 2019 IEEE Milan PowerTech, pp. 1–6.

Meeus, L., Belmans, R., 2008. Electricity market integration in Europe, in: 16th Power Systems Computation Conference 2008, p. 1505.

Mieth, R., Kim, J., Dvorkin, Y., 2020. Risk- and variance-aware electricity pricing. *Electric Power Systems Research* 189, 106804.

MOSEK ApS, 2021. MOSEK Modeling Cookbook. Documentation Release 3.2.3.

Pena, I., Martinez-Anido, C.B., Hodge, B.M., 2017. An extended IEEE 118-bus test system with high renewable penetration. *IEEE Transactions on Power Systems* 33, 281–289.

Roald, L., Oldewurtel, F., Van Parys, B., Andersson, G., 2015. Security Constrained Optimal Power Flow with Distributionally Robust Chance Constraints. *arXiv Preprint* 1508.06061. [arXiv:1508.06061](https://arxiv.org/abs/1508.06061).

Rte, Amprion, Creos, Elia, TenneT, TransnetBW, 2015. CWE Flow Based Market Coupling project: Parallel Run performance report.

Schavemaker, P., Croes, A., Otmani, R., Bourmaud, J.Y., Zimmermann, U., Wolpert, J., Reyer, F., Weis, O., Druet, C., 2008. Flow-Based Allocation in the Central Western European Region. Technical Report. Cigré.

Schönheit, D., Bruninx, K., Kenis, M., Möst, D., 2021a. Improved Selection of Critical Network Elements for Flow-Based Market Coupling Based on Congestion Patterns. Technical Report. ZBW – Leibniz Information Centre for Economics.

Schönheit, D., Dierstein, C., Möst, D., 2021b. Do minimum trading capacities for the cross-zonal exchange of electricity lead to welfare losses? *Energy Policy* 149, 112030.

Schönheit, D., Kenis, M., Lorenz, L., Möst, D., Delarue, E., Bruninx, K., 2021c. Toward a fundamental understanding of flow-based market coupling for cross-border electricity trading. *Advances in Applied Energy* 2, 100027.

Schönheit, D., Weinhold, R., Dierstein, C., 2020. The impact of different strategies for generation shift keys (GSKs) on the flow-based market coupling domain: A model-based analysis of Central Western Europe. *Applied Energy* 258, 114067.

Voswinkel, S., Felten, B., Felling, T., Weber, C., 2019. Flow-Based Market Coupling – What Drives Welfare in Europe’s Electricity Market Design? HEMF Working Paper No. 08/2019. University of Duisburg-Essen, House of Energy Markets & Finance.

Weinhold, R., Mieth, R., 2020a. Fast Security-Constrained Optimal Power Flow Through Low-Impact and Redundancy Screening. *IEEE Transactions on Power Systems* 35, 4574–4584.

Weinhold, R., Mieth, R., 2020b. Power Market Tool (POMATO) for the Analysis of Zonal Electricity Markets. *arXiv Preprint* 2011.11594v1.

Wyrwoll, L., Blank, A., Müller, C., Puffer, R., 2019. Determination of Preloading of Transmission Lines for Flow-Based Market Coupling, in: 2019 16th International Conference on the European Energy Market, pp. 1–6.